Been, B., Meijer, R., Bermond, F., Bortenschlager, K., Hynd, D., Martinez, L. & Ferichola, G. (2007). Worldsid small female side impact dummy specifications and prototype evaluation. In 20th International Technical Conference on the Enhanced Safety of Vehicles (ESV), 18-21 June, 2007, Lyon, France

WORLDSID SMALL FEMALE SIDE IMPACT DUMMY SPECIFICATIONS AND PROTOTYPE EVALUATION

Bernard Been
First Technology Safety Systems Europe
Riske Meijer
TNO Science & Industry
The Netherlands
Francois Bermond
INRETS - LBMC
France
Klaus Bortenschlager
PDB
Germany
David Hynd
TRL limited
United Kingdom
Luis Martinez
Gustavo Ferichola
University Institute for Automobile Research, Polytechnic University of Madrid (UPM-INSIA)
Spain
Paper Number 07-0311

ABSTRACT

The WorldSID program was set up to develop a new, worldwide acceptable, advanced technology, side impact crash test dummy for improved assessment of injury risk to car occupants in lateral collisions. Following the release of the mid-sized male WorldSID, the development of the small female WorldSID dummy was initiated by the EC 6th Framework collaborative research project 'APROSYS' in 2004.
The main specifications and requirements of the new dummy have been defined in terms of anthropometry, biomechanical response and instrumentation capabilities in general and per body segment. An overview of the specification is given in this paper. Two prototype dummies have been evaluated against a first set of test conditions. Test results are presented here, including pendulum impactor, linearly guided impactor, drop and sled tests. For a prioritised matrix of biomechanical test conditions, the dummy responses were compared against the biomechanical human response requirements. Furthermore, the dummy's repeatability in well-controlled test conditions and its sensitivity to temperature were studied and its compliance to anthropometric requirements is reported. Following the assessment of the dummy's current biofidelity and maturity, recommendations for further dummy improvements are given in the conclusions.

INTRODUCTION

In recent years there have been a number of developments in the field of side impact crash test dummy technology. The WorldSID 50th percentile male dummy was developed between 1997 and 2001 and evaluated against a number of biofidelity and sensitivity criteria.
After the development of the 50th percentile male dummy, the focus was put on the small (5th percentile) female size. The aim was to develop a dummy with the same biofidelity, functionality, handling and injury assessment capabilities as the WorldSID 50th percentile male dummy. The results of the WorldSID 50th percentile prototype testing were taken into account in the 5th female development. The specification of the WorldSID 5th female, including the selection of scaled biofidelity requirements, was undertaken in the Aprosys EC project (Barnes *et al.*, 2005). Five prototype dummies were built according to these specifications, two of which have been extensively evaluated in the Aprosys EC project.
This paper provides an overview of the biofidelity and anthropometry assessment of the dummy as well as assessment the dummy's repeatability, sensitivity to environmental temperature, its handling and robustness. The dummy's characteristics are evaluated against the requirements and recommendations are made as to potential improvements to the design and usability of the dummy to make it suitable for use in a regulatory test environment.

MAIN SPECIFICATIONS

The WorldSID small female requirements were published in a detailed document prepared in the Aprosys EC project (Barnes *et al.*, 2005). Further, the specifications of the WorldSID small female prototypes that were built according to these requirements were published by Wang *et.al.* (2007). The current paper only provides a brief overview of the main characteristics of the dummy.

Anthropometry

The small female WorldSID dummy was designed in order to represent a small-size adult female and adolescent car occupant. The dummy anthropometry was based on the UMTRI data set (Schneider *et al.*, 1983). This data set includes many anthropometry details for a small-sized female in an automotive seating posture, such as the external 3D surface, joint centre locations, external and internal anatomical reference points, and mass and inertia properties of the body segments. The dummy target mass is 45.8 kg ± 1.2 kg (~2.5%) including two half arms, excluding dummy suit and shoes.

Biofidelity

The biomechanical performance requirements of the WorldSID 5th female are based on impact responses as specified in ISO Technical Report 9790 (ISO, 1997) for lateral biofidelity, scaled for 5^{th} percentile female according the formulas specified by Irwin *et al.* (2002).
ISO Technical Report 9790 includes a large set of dynamic biofidelity performance specifications for the head, neck, shoulder, thorax, abdomen and pelvis of a 50^{th} percentile male side impact dummy in sled tests, drop tests and pendulum tests. This report includes a (weighted) biofidelity rating methodology that enables quantification of the ability of a certain dummy to meet the performance requirements. The target biofidelity rating for the WorldSID dummy family, including the small female, is to achieve "Good to Excellent Biofidelity", i.e. B ≥ 6.5 out of 10. The Irwin study gives scaling formulae and scaled responses for all body segments in all test conditions of ISO TR9790 for all available anthropometric sizes between a large 95^{th} percentile male down to new born child. The 5^{th} percentile female biofidelity response requirements as published by Irwin were applied to the 5th percentile female WorldSID dummy.

Instrumentation

The instrumentation options of the WorldSID 5^{th} female dummy are given in Table 1. A total of 125 dynamic measurement parameters are available in the dummy, completed with static measurements for tilt angle and temperature in head, thorax and pelvis.

Table 1.
Instrumentation options WorldSID small female

Segment	Parameter	Nr.
Head	Acceleration ($a_{x,y,z}$)	3
	Rotational acceleration ($\alpha_{x,y,z}$)	3
Neck	Upper loads ($F_{x,y,z}$, $M_{x,y,z}$)	6
	Lower loads ($F_{x,y,z}$, $M_{x,y,z}$)	6
Shoulder	Loads ($F_{x,y,z}$)	2*3
	Deflection (δ_y)	1
	Acceleration ($a_{x,y,z}$)	3
Thorax	T1 acceleration ($a_{x,y,z}$)	3
	T4 acceleration ($a_{x,y,z}$)	3
	T12 acceleration ($a_{x,y,z}$)	3
	Rib deflection (δ_y)	3
	Rib acceleration ($a_{x,y,z.}$)	3*3
	Rotational acceleration (α_x)	1
Abdomen	Deflection (δ_y)	2
	Acceleration ($a_{x,y,z}$)	2*3
Lumbar	Loads ($F_{y,z}$, $M_{x,z}$)	4
Pelvis	Sacro-iliac loads ($F_{x,y,z}$,$M_{x,y,z}$)	2*6
	Pubic loads (F_y)	1
	Acceleration ($a_{x,y,z}$)	3
	Rotational acceleration (α_x)	1
Femur	Femoral neck load ($F_{x,y,z}$)	2*3
	Femur load ($F_{x,y,z}$ $M_{x,y,z}$)	2*6
	Knee load (Fy)	2*2
Tibia	Upper load ($F_{x,y,z}$ $M_{x,y,z}$)	2*6
	Lower load ($F_{x,y,z}$ $M_{x,y,z}$)	2*6

EVALUATION METHOD

Anthropometry

The objective of this study was to determine actual dummy anthropometric details, such as joint-, landmark- and center of gravity locations; mass of body segments and total dummy, and external shape of the flesh components. Based on measured dummy dimensions, a complete and accurate CAD model was reconstructed by measuring components with a caliper, a FARO ARM 3D measurement machine and by digitising the external shapes of dummy flesh components. The actual components were weighed and the mass was applied to the CAD model components. The actual dummy was set up in the UMTRI reference position, using the internal tilt sensors of the dummy at zero tilt read out. Anthropometric reference points of the actual dummy assembly were measured with a FARO ARM and used to set up the reconstructed CAD model in 3D space. Centre of gravity (CoG) locations of actual dummy assemblies were obtained on a scale according Figure 1 and Equation 1.

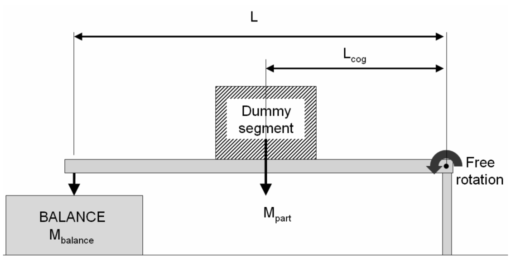

Figure 1. CoG location process.

$$L_{cog} = \frac{M_{balance} * L}{M_{part}} \qquad (1)$$

The reconstructed dummy CAD model was then analysed to obtain the dummy anthropometric characteristics, such as location of the joints, instrumentation and CoG and mass. Also the CAD model enabled comparison of the external shape of components in 3D space with the UMTRI "Golden Shell", the target outer surface of the small female anthropometry. The details obtained were compared to the UMTRI anthropometric targets and deviations between target and actual dummy anthropometric data were identified.

Biomechanical response

Test matrix - The test matrix for the biomechanical response evaluation of the small female WorldSID is given in Table 2. Note that the complete set of ISO TR9790 tests was not performed. In the ISO TR9790 rating system, test conditions and body segments are prioritised by weighting factors. The selection of test conditions for the Aprosys evaluation was based on the test condition weighting factors (V_{ij}), test severity and available skill and equipment within the Aprosys consortium. Drop tests, low weighting factor tests and high risk tests (in terms of dummy damage) were omitted.

Table 2.
Prioritised test matrix Aprosys

Body region	Impact condition	V_{ij}
Head		
Head test 1	200 mm rigid drop	8
Frontal drop	376 mm rigid drop	0
Neck		
Neck test 1 shoulder test 2	7.2 g sled impact	7
Neck test 2	6.7 G sled impact	6
Shoulder		
Shoulder test 1	4.5 m/s pendulum	6
Shoulder 4, Thorax 6, Abdomen 5, pelvis 13	8.9 m/s padded WSU	7
Thorax		
Thorax test 1	lateral 4.3 m/s pendulum	9
Thorax test 2	oblique 6.7 m/s pendulum	9
Thorax test 5 pelvis 7	6.8 m/s Heidelberg rigid sled	7
Abdomen		
Abdomen test 3	8.9 m/s WSU padded sled	3
Pelvis		
Pelvis test 1	6.0 m/s impactor	8
Pelvis test 2	10 m/s impactor	9
Pelvis test 9 thorax 6	8.9 m/s Heidelberg padded sled	8
Pelvis test 10	6.8 m/s WSU rigid sled	3

Sled velocity - The EEVC Heidelberg test procedure (Roberts *et al.*, 1991) specifies the dummy to load cell wall impact velocity as 7.6 and 10.3 $m.s^{-1}$, rather than the sled velocity of 6.8 and 8.9 $m.s^{-1}$ used in the ISO TR9790 documentation. The difference is because the EEVC analysis used the relative speed of impact between the dummy and the load plates (which included the rebound velocity of the sled), and the ISO analysis used only the velocity of the sled at t_0. Note that there is no difference in the actual loading condition between ISO and EEVC. Therefore the data obtained in these tests can be analysed applying EEVC as well as ISO corridors. However, when applying sled velocity as test parameter in a rebounding sled (e.g. Heidelberg), the dummy to load plate contact velocity is likely to be less accurately controlled as it will depend on the performance of the sled deceleration and stopping mechanism.

Scaling of force plates - To achieve similar force plate interaction with the small female dummy as the original PMHS test set up, the force plates in both sled test conditions - Heidelberg and Wayne State University (WSU) - were scaled using the same method. The vertical scale factor was determined from the ratio between Occiptal Condyle joint to seat pan distance of small female and mid size male, resulting in scale factor of 0.895. Both the location of the beams and the height of the beams were scaled in a direction perpendicular to the seat pan. The scaled and original beam locations are illustrated in Figure 2 for the WSU configuration. To calculate the location of the knee plate and the dimension of the pelvis beam a scale factor of 0.917 was applied. The scale factor is based on ratio of the UMTRI 5^{th} and 50^{th} femur lengths.

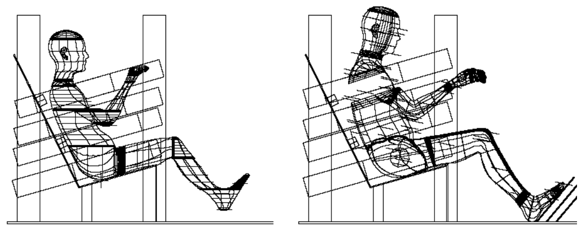

Figure 2. WSU beam configurations and human body models. Left 5^{th} % female, right 50^{th} % male.

Normalisation - The dummy responses were normalised according the procedures used for normalising PMHS raw data to obtain ISO TR9790 and EEVC response corridors. The small female standard mass was determined using the ISO standard body segment mass (50^{th} male) per test condition scaled by the ratio of UMTRI body segment mass 5F/50M. No stiffness scaling was applied as ratios of characteristic lengths of the dummy equal 1

.

Pendulum tests - The effective mass in each test was calculated using Equation (2):

$$M_e = \frac{\int F dt}{V_0} \qquad (2)$$

Where M_e = effective mass of the segment (kg);
F = pendulum force (N);
V_0 = pendulum velocity ($m.s^{-1}$).

The integration interval was taken to be from first positive pendulum force to the end of the impact.

The shoulder and pelvis pendulum forces were normalised according to Equation (3):

$$F_N = F_p \sqrt{\frac{M_s}{M_e}} \quad (3)$$

where F_N = normalised pendulum force (N);
F_p = pendulum force (N);
M_s = standard segment mass (kg);
M_e = effective segment mass (kg).

The shoulder displacement was normalised according to the Equation (4):

$$D_N = D_s \sqrt{\frac{M_s}{M_e}} \quad (4)$$

where D_N = normalised deflection (mm);
D_s = measured shoulder deflection (mm).

The thoracic pendulum responses were normalised using the two mass system methods as applied in ISO TR9790 according to Equation (5). Time factor scaling was applied to the HSRI and WSU/GML thoracic pendulum responses according Equation (6). The T1 acceleration responses in the 4.3 m/s HSRI thorax tests were normalised according Equation (7).

$$F_N = F_p \sqrt{\frac{M_s}{M_e}} \times \sqrt{(14 + M_e)} / \sqrt{(14 + M_s)} \quad (5)$$

$$t_N = t_p \sqrt{\frac{M_s}{M_e}} \times \sqrt{(14 + M_e)} / \sqrt{(14 + M_s)} \quad (6)$$

$$a_N = a_{T1} \sqrt{\frac{M_e}{M_s}} \times \sqrt{(14 + M_e)} / \sqrt{(14 + M_s)} \quad (7)$$

where t_N = normalised time (s);
a_N = normalised T1 acceleration (G);
a_{T1} = T1 acceleration (G);
14 = the pendulum mass (kg).

Shoulder - The APR lateral shoulder tests were normalised using a standard mass of 20.5 kg. 5th %-ile UMTRI shoulder-thorax segment mass is 12.983 kg, 50th %-ile UMTRI shoulder-thorax segment mass is 23.763 kg. The 5th female standard shoulder mass Ms = 20.5*12.983/23.763 = 11.20 kg. The average effective mass Me in three tests was 12.663 kg. The shoulder normalisation factor applied was 0.940 for both pendulum force and deflection.

Thorax - The HSRI lateral thorax tests were normalised using a standard mass of 20.8 kg for the thorax. 5^{th} %-ile UMTRI shoulder-thorax segment mass is 12.983 kg and 50^{th} %-ile UMTRI shoulder-thorax segment mass is 23.763 kg. The 5^{th} female standard shoulder mass M_s = 20.8*12.983/23.763 = 11.364 kg. The average effective mass M_e in three 4.3 m/s tests was 13.351 kg. The thorax 4.3 m/s normalisation factor applied was 0.958. The WSU/GMR lateral thorax tests were normalised using a standard mass of 15.2 kg for the thorax. 5^{th} %-ile UMTRI shoulder-thorax segment mass is 12.983 kg and 50^{th} %-ile UMTRI shoulder-thorax segment mass is 23.763 kg. The 5^{th} female standard thorax mass M_s = 15.2*12.983/23.763 = 8.305 kg. The average effective mass M_e in three 6.0 m/s tests was 12.988 kg. The thorax 6.0 m/s normalisation factor applied was 0.880.

Pelvis - The pelvis pendulum tests were run with a 14 kg mass and the linear guided impactor tests were performed with a 10.26 kg mass. The prescribed pendulum mass is 10.14 kg for small female pelvis impacts. The data were scaled applying scale factor according Equation (8):

$$F_p = F_{imp} * \sqrt{(10.14 * (M_i + 48)} / (M_i * (10.14 + 48)) \quad (8)$$

where M_i = mass of impactor used in the test (kg);
F_{imp} = impactor force (N).

As second step the data were normalised following the ONSER lateral pelvis tests according to Equation (2) and (3). A standard mass of 14.5 kg was applied for the pelvis. 5^{th} %-ile UMTRI pelvis segment mass (including femur heads) is 8.5 kg and 50^{th} %-ile UMTRI pelvis segment mass (including femur heads) is 14.5 kg. The 5^{th} female standard pelvis mass applied was M_s = 14.5*8.5/14.5 = 8.5 kg.

Sled tests - In the Heidelberg tests the force plates were mounted on the sled. Therefore the readings were inertia compensated as follows:

$$F_i = F_{plate} + (M_{plate} \text{ x } A_{plate}) \quad (9)$$

Where F_i = inertia compensated plate force (N);
F_{plate} = sum of plate load cell forces (N);
M_{plate} = mass of plate forward of the centre of the load cells (kg);
A_{plate} = acceleration of plate, where acceleration is positive in the direction of impact of the dummy ($m.s^{-2}$).

The WSU force plates were mounted statically and no inertia compensation was applied. The Heidelberg inertia compensated and WSU registered plate forces were normalised according to Equation (10).

$$F_N = F_i \sqrt{\frac{M_s}{M_e}} \quad (10)$$

where F_N = normalised wall force (N);
F_i = inertia compensated force

Dummy measurements were normalised according to the Equations (11), (12) and (13).

$$F_N = F_i \sqrt{\frac{M_s}{M_e}} \quad (11)$$

$$x_N = x_i \sqrt{\frac{M_s}{M_e}} \quad (12)$$

$$A_N = A_i \sqrt{\frac{M_e}{M_s}} \quad (13)$$

where x_N = normalised displacement (m);
x_i = displacement (m);
A_N = normalised acceleration ($m.s^{-2}$);
A_i = acceleration ($m.s^{-2}$).

Standard mass - For Heidelberg sled tests, EEVC normalisation applied a 37 kg segment mass for the thorax and 24 kg for the pelvis. The ISO normalisation used a 38 kg thorax segment and the whole dummy mass to normalise the pelvis responses. The ratio of the 5^{th} to 50^{th} %-ile total body masses was used to scale all segment masses to 23.5kg thorax mass and 15.2 kg pelvis mass for the EEVC and 24.1 kg thorax for ISO. A ratio of specified 5^{th} %-ile mass to actual dummy mass was used in the ISO normalisation of the pelvis responses. In the Wayne State University sled tests small female standard masses were applied as follows: thorax 15.2 kg, abdomen 6.7 kg and pelvis 10.8 kg.

RESULTS

Anthropometry

Segment mass - The target body segment masses and those obtained for WorldSID 5^{th} female are given in Table 3. Note that the WorldSID masses given are from (not necessarily functional-) sub-assemblies that match UMTRI segmentation planes as closely as possible. The CAD model and UMTRI segmentation planes are shown in Figure 3. The main deviations are in abdomen (-1.3 kg) and lower legs and feet (+1.2 kg). The other large deviation of 2.5 kg in the pelvis/upper leg is due to the mismatch between the UMTRI segmentation plane and dummy components. The dummy pelvis extends forward of the UMTRI segmentation plane and contains a large portion of the thigh. The overall dummy mass is well within the tolerance specification.

Table 3.
Target and dummy body segment mass [gram]

Body segment	UMTRI	WorldSID 5^{th}	Deviation
Head	3697	3660	-37
Neck	601	541	-60
Thorax including only upper arms	15231	15452	222
Abdomen	1610	305	-1305
Pelvis	6976	9475	2499
Upper legs	11828	9160	-2668
Lower legs	4720	5486	766
Feet	1276	1724	448
Total	**45939**	**45804**	**-135**

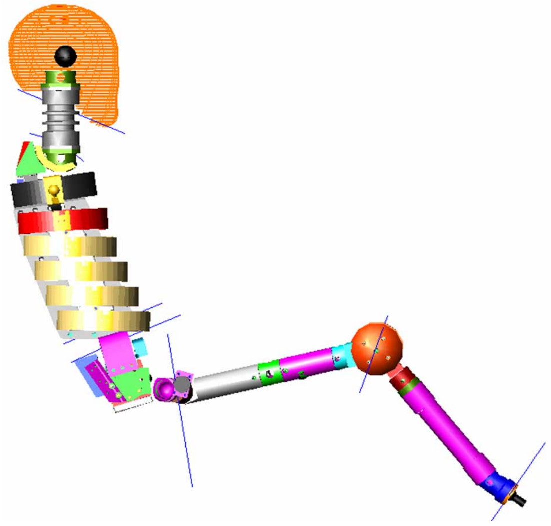

Figure 3. Reconstructed CAD model and UMTRI segmentation planes.

Table 4.
Target and dummy centre of gravity [mm]

	UMTRI			WorldSID 5^{th}		
Body segment	X	Y	Z	X	Y	Z
Head	-184	0	578	-177	-1	580
Neck	-172	0	460	-185	1	446
Thorax	-147	0	238	-170	-1	258
Pelvis	-76	0	25	-36	0	19
Upper leg	147	±104	-4	232	±92	38
Lower leg	444	±82	-56	491	±83	-81
Feet	653	±101	-178	654	±93	-171
Whole body	24	0.0	129	48	-0.5	136

Centre of Gravity - The target and dummy centres of gravity are shown in Table 4 and Figure 4. The black balls represent target CoG's and the green balls the CoG of the dummy segments.
Main deviations are found in the thorax: +20 mm in vertical and horizontal direction. The whole body

CoG is too far forward and the dummy lower legs CoG are too far backward and too high up. The high thorax CoG is due to the low abdomen mass. The forward position of the whole body CoG is due to the high mass in the lower leg and feet. Redistribution of these masses would bring the whole body CoG and the thorax CoG closer to the targets. There is also a deviation in the pelvis and upper leg in the X direction. This deviation is due to the segmentation plane deviation between dummy and UMTRI. This is not a problem with the dummy.

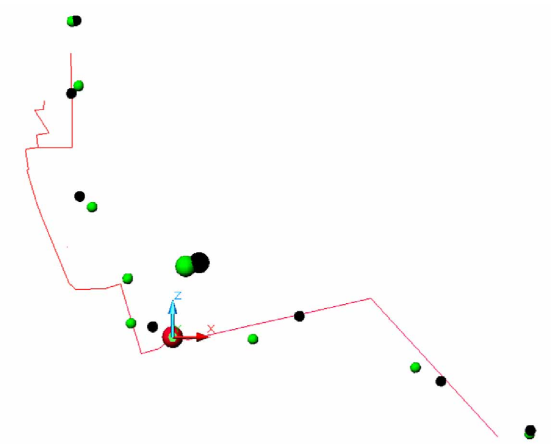

Figure 4. Target (black) and dummy (grey) centre of gravity.

Table 5.
UMTRI targets and dummy joint locations [mm]

	UMTRI			WorldSID		
	X	Y	Z	X	Y	Z
OC	-189	0	519	-187	-1	519
T1	-183	0	429	-184	1	424
Shoulder	-174	±146	354	-194	±147	348
T12/L5 joint	-149	0	140	-86	0	67
L5/S1 joint	-80	0	46	-86	0	67
H-point	0	0	0	0	0	0
Hip	0	±80	0	0	±80	0
Knee	363	±75	71	362	±75	71
Ankle	593	±86	-182	594	±86	-182

Joint locations - The UMTRI target and dummy joint locations are given in Table 5. The dummy was seated with 0º angle tilt sensor reading for this study. The table shows that there is a very good match between the dummy posture and the UMTRI reference posture. Deviations are found in the shoulder joint (rearward 20mm). This is a deviation by design, as the dummy construction did not allow matching the shoulder joint target entirely. The downward (-6mm) position of the shoulder joint may have to do with slight sagging of the shoulder rib due to the arm weight and/or the compression of the lumbar spine. The latter is confirmed by slightly low T1 position. However the OC joint precisely matches the vertical target. The lumbar joint does not match the human targets by design. The dummy lumbar spine is much shorter than human because of design constraints. In the analyses the mid point of the lumbar component was assumed as the joint location, therefore the same numbers appear twice for dummy T12/L5 and L5/S1 joints in the table.

Outer surfaces - A comparison of the outer surface of UMTRI and the reconstructed CAD model (Figure 5) shows a very good match between the two. However some deviations appear as well. First of all the abdomen ribs are wider than the UMTRI target. The thorax and abdomen ribs were designed to be the same width on purpose to avoid discontinuity, which was anticipated to give response or sensitivity problems. A further rationale is that the dummy should not only represent 5th percentile females, but also adolescent males (13 year old). Further deviations are found in T1, clavicle and the knee area. These are all known design compromises. Close study also reveals deviation at the foot surface, but this is considered a minor issue. Figure 6 shows a deviation between the dummy half arm and bone which are much shorter than their UMTRI targets. This deviation appears as a problem in the sled tests; see abdomen responses, page 11.

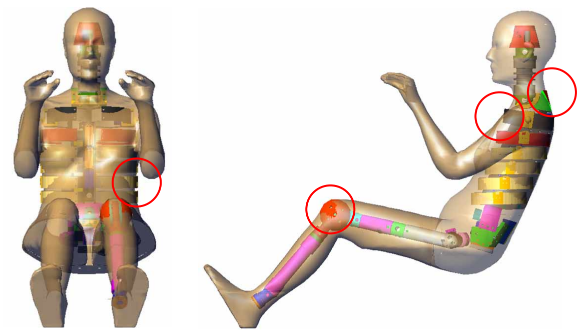

Figure 5. Reconstructed CAD model inside UMTRI 5th female "Golden Shell" surface model.

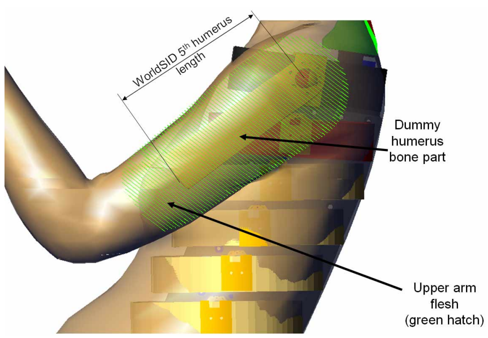

Figure 6. Dummy upper arm and humerus profile.

Biomechanical response

In the following chapters the results will be discussed per body segment rather than per test condition to allow making body segment conclusions based on multiple test conditions.

Head - The results of the head drop tests are given in Table 6. In the original PMHS tests the head impact accelerations were measured directly on the skull; on a point on the non-struck side of the head coincident with a lateral axis through the head CoG. To match the PMHS response, the dummy acceleration results at the non-struck side of the head were calculated from the linear and rotational accelerations measured at the head CoG. The equations are given in (Wang *et al.*, 2007). Note that the frontal head response is just below the corridor and the lateral response is within the corridor. As the ISO TR9790 only applies a lateral performance requirement, the head biofidelity achieved a 10 rating.

Table 6.
Results head drop tests [G]

Condition	Resultant acceleration [G]		Corridor	Criteria
	CoG	Side		
Lateral	120.1	139.5	107-161	pass
Lateral	118.9	135.9		pass
Frontal	244.2	NA	250-300	fail
Frontal	235.7	NA		fail

Neck - The WorldSID small female head-neck responses to NBDL and Patrick and Chou (P&C) conditions are presented in Figure 7 through Figure 16. Four tests were performed with different belt configurations to optimise the dummy T1 acceleration (Figure 15). The traces are differentiated by colours as follows: *black* tight 5-point belt with lateral torso belt; *blue* tight 5-point belt; *magenta* slack 5-point belt; *green*: slack 5-point belt and 30 mm shoulder panel gap. The latter test is considered not valid, because in the original NBDL tests there was no gap. In the graphs ISO corridors appear in *red*; derived corridors from P&C appear *red dotted*.

The internal neck loads of the NBDL tests were derived as explained in Philippens *et al.* (2004).

The plots are arranged such that NBDL and P&C responses can easily be compared. The responses of the same parameters are plotted next to each other, NBDL on the left and P&C on the right. Note that the scales of the left-hand and right-hand plots are identical. Presenting the plots this way shows that the head responses to the two test conditions are strikingly similar. Although pulses are different in NBDL and P&C, it appears that the neck acts as a mechanical filter and head responses are very similar. A noticeable difference is the slower response in NBDL. Also differences appear in the T1 response, see Figure 15and Figure 16. Considering the striking similarity (for this dummy, but possibly others as well) between head responses, there appears to be an incompatibility between NBDL and Patrick and Chou head - neck response requirements. This is demonstrated by the good performance of the dummy in the NBDL condition and the poor result in the P&C condition, see Table 7.

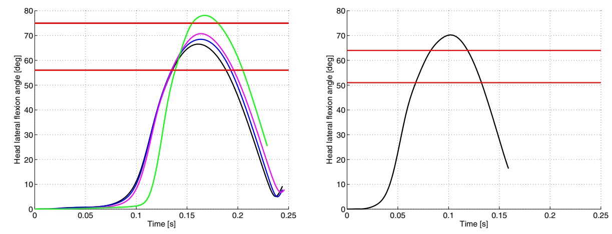

Figure 7. Head flexion angle NBLD (L), P&C.

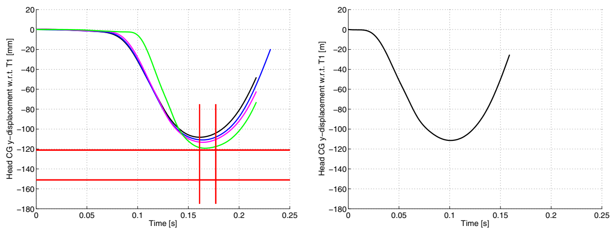

Figure 8 Head y-displacement NBLD (L), P&C.

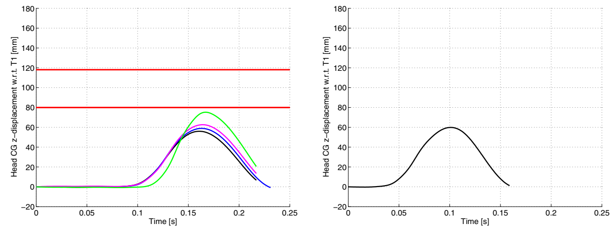

Figure 9. Head z-displacement NBLD (L), P&C.

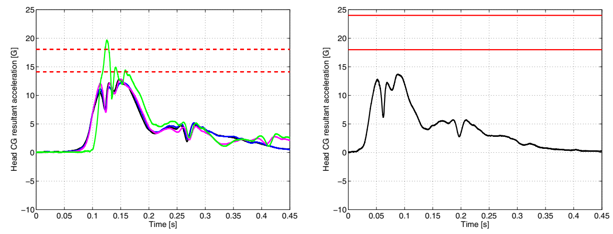

Figure 10. Head resultant acceln. NBLD(L), P&C.

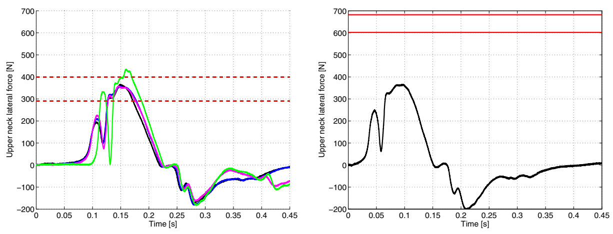

Figure 11. Head y OC force NBLD (L), P&C.

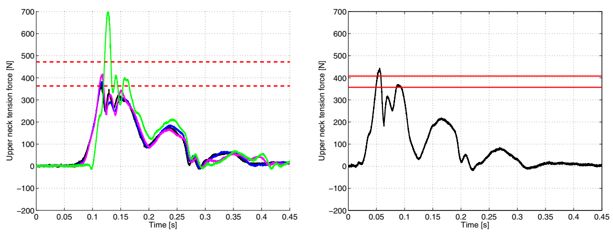

Figure 12. Head z OC force NBLD (L), P&C.

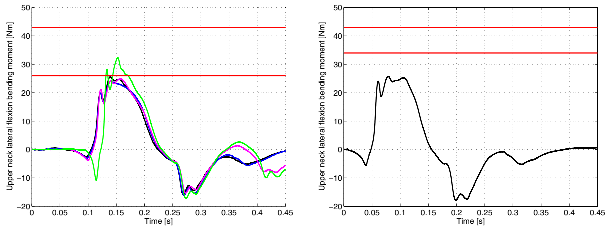

Figure 13. OC-x moment NBLD (L), P&C.

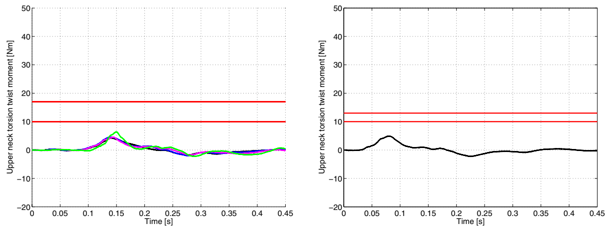

Figure 14. OC-z moment NBLD (L), P&C.

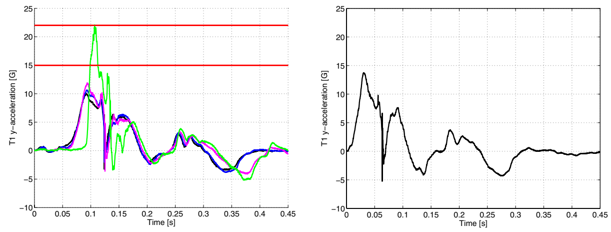

Figure 15. T1 y-acceleration NBLD (L), P&C.

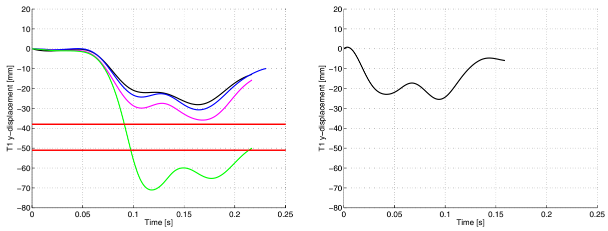

Figure 16. T1 y displacement NBDL (L), P&C.

The head and neck NBDL and P&C response requirements were further analysed for compatibility. The head lateral flexion angle should lie between 56 - 75° for NBDL and 51 - 64° for P&C. The overlapping corridor between NBDL and P&C is quite narrow (60° ± 6.6%). The NBDL resultant head acceleration can be calculated from NBDL a_y and a_z corridors and the mean a_x volunteer response reported in ISO TR9790 (6G). Doing so, the head resultant acceleration NBDL Head A_{res} 14 - 18G is not compatible with the P&C Head A_{res} 18 - 26G requirement. For free body motion such as a dummy head and neck, the neck loads and head acceleration have a direct correlation as long is there is no external force acting on the head. The neck loads can be derived from the product of head acceleration and head mass. Applying this simple equation allows comparison of NBDL vertical and lateral accelerations with P&C vertical and lateral neck loads. Using 3.7kg head mass, NBDL F_y 290 - 400N and P&C F_y 602 -682N. NBDL and P&C lateral head response requirements are completely incompatible. NBDL F_z 363 - 472N, P&C F_z 357 - 408N; vertical head response requirements are partly overlapping with a narrow corridor (385N ± 5.8%). The corridors for OC-x and OC-z moment are rather similar for NBDL and P&C, however NBDL are wider, as they are based on a larger data sample size (P&C is based on a single volunteer).

Table 7.
Neck ISOTR9790 biofidelity rating

Impact condition	Measurement	Average	Test	Body region
7.2 g sled impact NBDL	Peak horizontal Acc T1	5.0		
	Peak hor. Displ. T1/sled	5.0		
	Peak hor. Displ. head cg/t1	5.0		
	Peak vert. Displ. Head CG/T1	5.0		
	Time of max head excursion	10		
	Peak lateral Acc head cg	10		
	Peak vertical Acc head cg	8		
	Peak flexion angle	10		
	Peak twist angle	0.0		
	Peak OC lateral bending moment	6.7		
	Peak OC torsion twist moment	5.0		
			6.6	
6.7 G sled impact Patrick & Chou	Peak flexion angle	5.0		
	Peak bending X-moment @ OC	5.0		
	Peak bending Y-moment @ OC	0		
	Peak twist Z-moment	0		
	Peak shear PA (FX) @ OC	0		
	Peak FY @ OC	0		
	Peak FZ tension @ OC	5.0		
	Peak res. Acc. Head CG	5.0		
			2.9	
				4.9

Shoulder - The shoulder response was evaluated under three test conditions: the APR shoulder pendulum tests at 4.5 m/s, the NBDL 7.2 G sled impact and the WSU 8.9m/s padded sled impact on a load plate. The results are plotted in Figure 15 through Figure 19. In the APR pendulum tests the responses were normalised. The pendulum force exceeds the corridor slightly and the deflections stay below the corridor. The shoulder ISO rating for this test is 5. In the NBDL 7.2 G sled impact responses one clear outlier is visible, which was obtained with shoulder panel gap. This test is not valid. In NBDL the volunteer and dummy responses were not normalised. The T1 acceleration and the deflection are below the corridor. ISO rating for this test is 5.

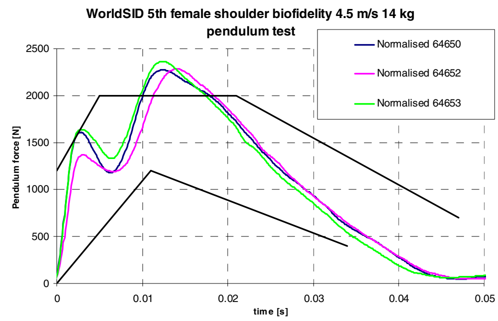

Figure 17. Pendulum force shoulder impact.

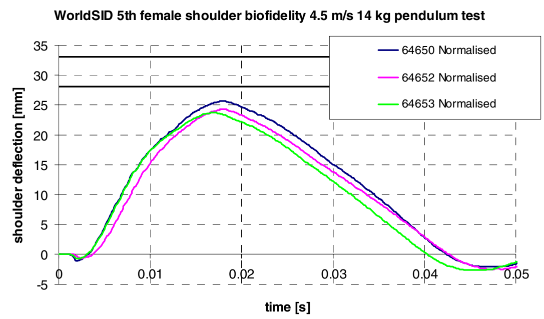

Figure 18. Shoulder deflection pendulum test.

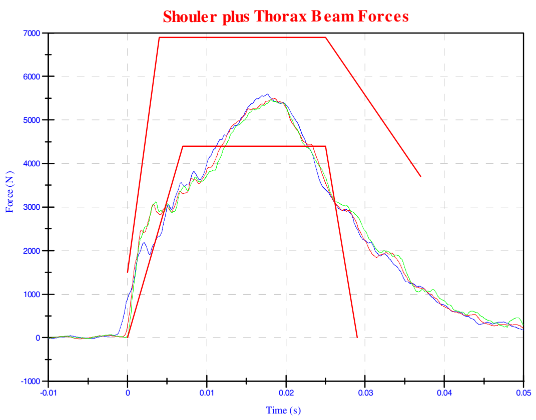

Figure 19. WSU 8.9 m/s padded shoulder and thorax force.

In the WSU 8.9 m/s padded sled impact the shoulder and thorax beam force is inside the upper corridor and the lower boundary is crossed. The response is very close to scoring 10 points in the ISO TR9790 rating. The overall shoulder biofidelity is 5.0 considering the three test conditions (out of four specified), see Table 8.

Table 8.
Shoulder ISOTR9790 biofidelity rating

Impact condition	Measurement	Average	**Test**	**Body regio**
4.5 m/s APR pendulum	Pendulum force-time Pendulum Force Peak shoulder deflection	5.0 5.0	**5.0**	
7.2 G sled sled NBDL	Peak horizontal Acc T1 Peak hor. Displ. T1/sled	5.0 5.0	**5.0**	
8.9 G WSU sled 23 PSI padded	shoulder + thoracic plate force	5.0	**5.0**	
				5.0

Thorax - The thorax biofidelity was evaluated in two pendulum and two sled test conditions. The results are shown in Figure 19 through Figure 23. All graphs show the same trend: the force responses are (almost) entirely inside the corridors. In some cases the lower boundaries are crossed and the duration of the response is on the short side; however, this was not confirmed in the Heidelberg 6.8 m/s rigid thorax response. The responses are very close to scoring 10 points in the ISO TR9790 rating. Slight lower corridor crossing was also visible in the PMHS original tests. The T1 acceleration is too high in the 4.3 m/s pendulum tests. The lower spine displacement in the padded 8.9 m/s WSU sled condition was inside the corridor in all three repeat tests.

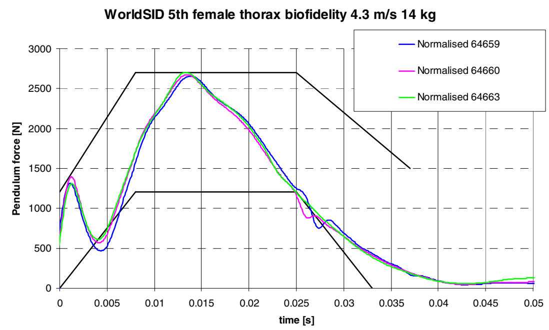

Figure 20. 4.3m/s 14kg thorax pendulum force.

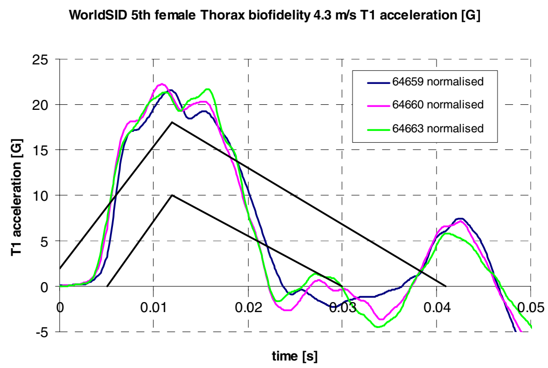

Figure 21. 4.3m/s 14kg thorax T1 acceleration.

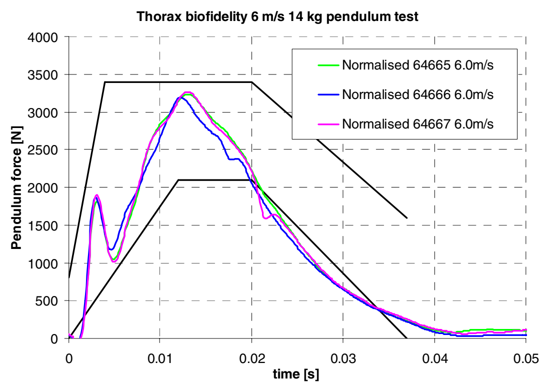

Figure 22. 6.0m/s 14kg thorax pendulum force.

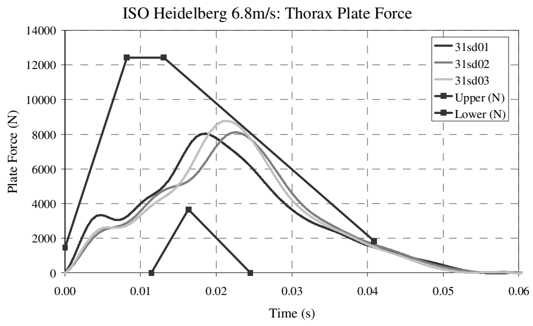

Figure 23. 6.8m/s Heidelberg thorax force ISO.

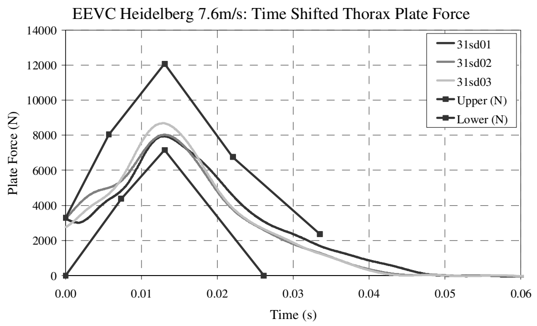

Figure 24: 6.8m/s Heidelberg thorax force EEVC.

The acceleration responses in the Heidelberg test are given in Table 9. Note that dummy rib1 corresponds with human rib4. The T1 and T12 spine responses are below the ISO targets, while the rib accelerations are above the ISO targets. Such response suggests that there may be a mass distribution problem, with too little mass on the outer circumference of the dummy and too much mass in the spine. This hypothesis is further supported considering that this dummy does not have damping material on the ribs, that the ribs themselves are made from a relatively low density alloy, and there is not much more material outside the ribs than a foam pad and a dummy suit. However the T1 acceleration in the 4.3 m/s pendulum test contradicts this hypothesis.

Table 9.
Peak lateral accelerations 6.8 m/s rigid sled test

Peak Lateral acceleration	ISO target	test1	test2	test3	CV %
T1	100-149	54.5	50.3	54.2	5.1
Rib 1	78-122	176	159	155	6.7
T12	87-131	54.6	53	63.9	10.3

The overall thorax responses are summarised in Table 10. The force-time responses of three tests are very close to scoring 10 points in the ISO TR9790 rating. The good performance of the thorax body segment is not fully reflected in the body segment rating of 6.3 according ISO TR9790. Note that this score is based on sub set of four out of six specified test conditions.

Table 10.
Thorax ISOTR9790 biofidelity rating

Impact condition	Measurement	Average	Test	Body region
4.3 m/s HSRI pendulum	Pendulum force	5.0		
	Peak T4 Y acc.	5.0	**5.0**	
6.0 m/s WSU/GML pendulum	Pendulum force	5.0	**5.0**	
6.8 m/s Heidelberg rigid sled	Thorax plate force	10		
	peak T1 Y acc.	3.3		
	peak T12 Y acc.	5.0		
	peak rib acc.	5.0	**6.0**	
8.9 m/s WSU sled 23 PSI padded	shoulder + thoracic plate force	5		
	Peak lateral displacement of T12	10	**6.8**	
				5.6

Abdomen - The abdomen biofidelity is evaluated in two Wayne State University sled test conditions at 6.8 m/s rigid and 8.9 m/s padded. The responses are shown in Figure 25 and Figure 26, the biofidelity rating is given in Table 11. The abdomen force is almost entirely in the corridor for the 6.8 m/s test and fully within the envelope of the 8.9 m/s test. The abdomen response, rated 8.5 in these tests, is rather good; however, only two out of five test conditions are considered for the abdomen.

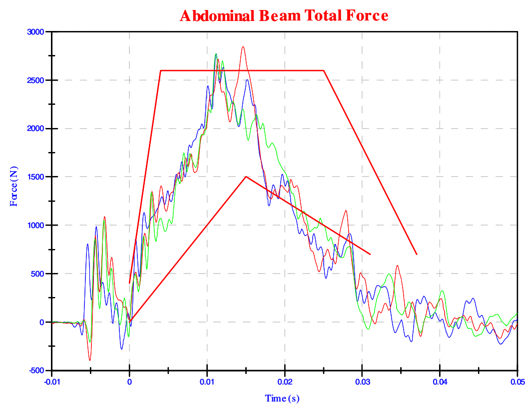

Figure 25. Abdomen force 6.8 m/s rigid WSU.

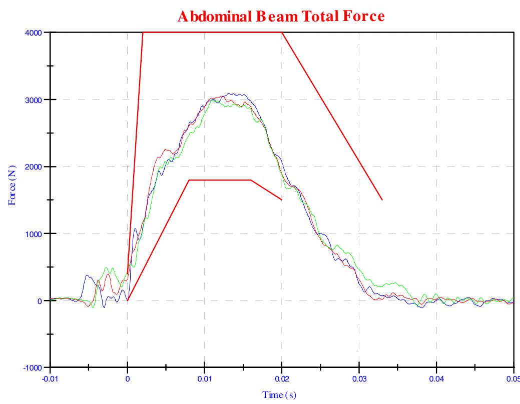

Figure 26. Abdomen force 8.9 m/s padded WSU.

Table 11.
Abdomen ISOTR9790 biofidelity rating

Impact condition	Measurement	Average	Test	Body regio
6.8 m/s WSU rigid sled	Abdominal plate force	5.0	**5.0**	
8.9 m/s WSU sled 23 PSI padded	Abdominal plate force	10	**10**	
				8.5

One particular outcome of the abdomen test was the poor repeatability of abdomen deflection in the sled tests (CV 23%) and the significant difference between upper and lower abdomen deflection, see Table 15. During the anthropometry evaluation it was found that the upper arm length did not meet the anthropometric target, see Figure 6. Figure 27 shows the position of the WorldSID small female on the sled and the relative position to the force beams. Note that the arm is in-between the torso and the load plates of the sled. The figure shows that lower end of the arm is coincident with the top of the lower abdomen and that the lower abdomen is not loaded through the arm. The unbalanced loading of the upper/lower abdomen in case the arm is in the load path, raises a concern of over-/under-assessment of injury. The other concern raised is that the interaction of the dummy with the load plate was different than the PMHS in the original tests. The poor repeatability of the lower abdomen is due to the small interaction with the load plate, resulting in small deflection and the relatively large influence of small variations. A second factor may be that, due to a small variation in arm position, there was more interaction with the arm in one test than in the other tests.

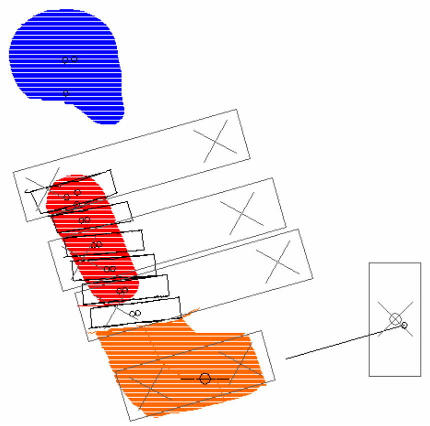

Figure 27. WorldSID small female position relative to WSU load plates.

Pelvis - The biofidelity of the pelvis was evaluated in seven test conditions, five of which were rigid and padded sled tests and two were linear guided and pendulum impactor tests. The linear guided impactor tests were performed with a mass of 10.26kg and the pendulum impactor tests were performed with a 14kg pendulum. The responses of the impactor tests were scaled to 10.14kg, using Equation (8).
The pelvis sled test responses are presented in Figure 28 through Figure 30 and Table 12. The responses are shown relative to EEVC as well as ISO corridors. The pelvis performs particularly well in the high speed padded and rigid sled tests and the low speed impactor tests. In these tests the force responses are inside the corridors. The acceleration responses are close to the corridors; the rigid Heidelberg accelerations are too high (high and low speed), WSU and Heidelberg high speed padded and WSU rigid low speed accelerations are below the corridors. No trend can be found in the pelvis accelerations.

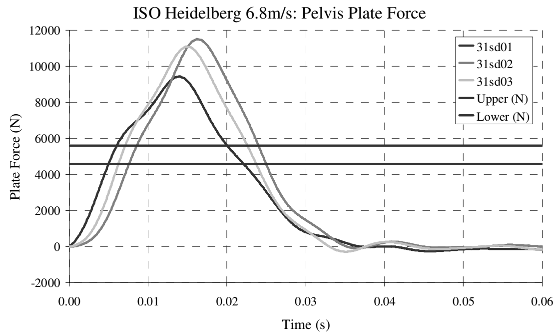

Figure 28. Pelvis Heidelberg 6.8 m/s rigid ISO

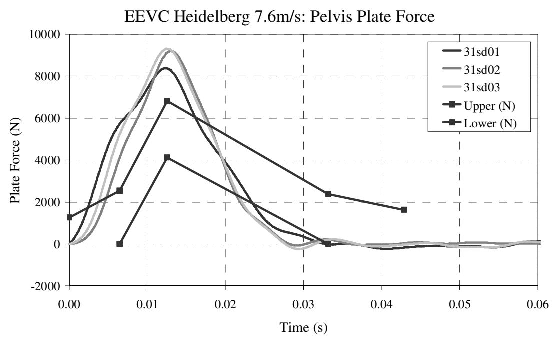

Figure 29. Pelvis Heidelberg 7.6m/s rigid EEVC.

The performance in the WSU 6.8 m/s rigid and the high speed impactor tests is reasonable. The performance is poor in the low speed rigid Heidelberg test in the ISO corridors and slightly better according EEVC corridors. No trend can be obtained from the pelvis force responses relative to impact velocity, as sled test and impactor tests show a contradicting trend. The different responses between tests may be explained by the different loading: in the impactor test the pelvis is loaded locally at the Greater Trochanter, in the Heidelberg tests all of the thigh and pelvis is loaded and in WSU only half of thigh is loaded and there is a knee impact plate.

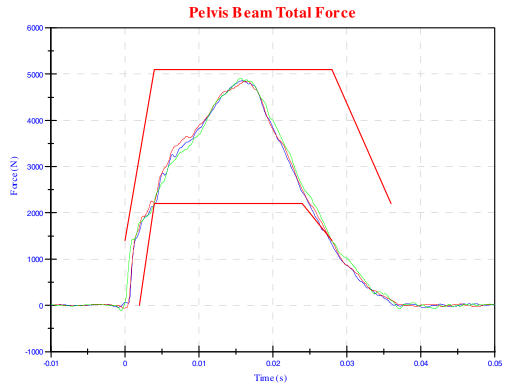

Figure 30. Pelvis WSU 8.9m/s padded

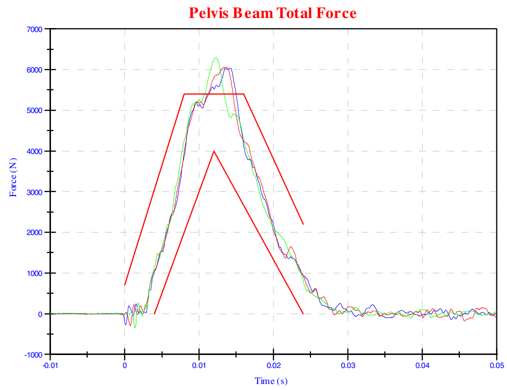

Figure 31. Pelvis beam force WSU 6.8m/s rigid ISO corridors

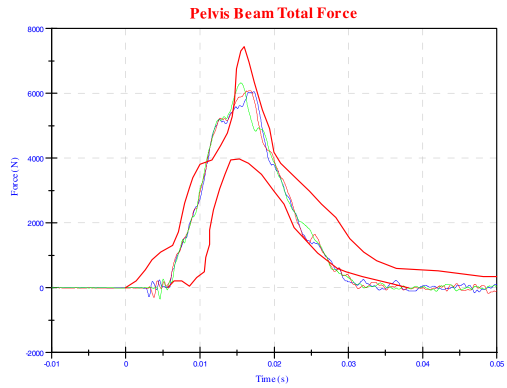

Figure 32 Pelvis beam force WSU 6.8m/s rigid EEVC corridors

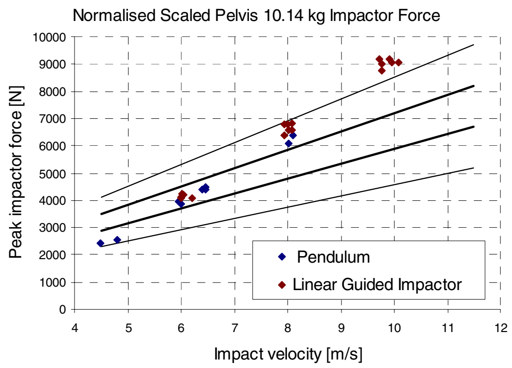

Figure 33. Normalised pelvis impactor forces

Table 12.
Summary pelvis sled test results

		Corridors		test1	test2	test3	CV%
Heid 6.8R	force	4.6	5.6	9.3	11.3	10.9	10.1
	acc.	78	95	99.3	101	102	1.2
Heid 8.9R	force	16.2	19.1	16.8	17.8	17.3	2.9
	acc.	118	143	162	166	164	2.7
Heid 8.9P	force	8.4	9.8	9.3	9.6	9.6	1.8
	acc.	75	93	68.2	71.9	70.5	2.7
wsu 6.8R	force	4	5.4	6.0	6.1	6.3	3.7
	acc.	105	142	101	96.2	102	1.7
wsu 8.9P	force	2.2	5.1	4.9	4.8	4.9	1.2
	acc.	80	110	76.6	76.7	74.3	1.8

Table 13.
Pelvis ISOTR9790 biofidelity rating

Impact condition	Measurement	Aver age	Test	Body regio
4.5 m/s 10.14 kg impact	Pendulum force	10	10	
11.5 m/s 10.14 kg impact	Pendulum force	0	0	
6.8 m/s Heidelberg rigid sled	Peak pelvic force Peak pelvic acc.	0.0 5.0	2.2	
8.9 m/s Heidelberg rigid sled	Peak pelvic force Peak pelvic acc.	10 5.0	7.7	
8.9 m/s Heidelberg padded sled	Peak pelvic force Peak pelvic acc.	10 5.0	7.6	
6.8 m/s WSU rigid sled	Peak pelvic force Peak pelvic Y acc.	5.0 5.0	5.0	
8.9 m/s WSU 23 PSI padde sled	Peak pelvic force Peak pelvic Y acc.	10 5.0	7.8	
				5.6

The ISO TR9790 pelvis biofidelity rating per test condition and overall is summarised in Table 13. The table shows some very good and some poor results, but does not clearly indicate how to improve further the pelvis segment biomechanical response. The overall pelvis biofidelity rating is 5.6 and does not meet the body segment target of ‘good to excellent’ biofidelity. Note that this score is based on sub set of seven out of thirteen specified test conditions; however the highest weighting factor tests were included in this sub set.

Biofidelity

The body segment and full dummy biofidelity is summarised in Table 14. The result is based on a sub-set of test conditions with high weighting factors and is a good indication of the dummy’s biofidelity. The overall rating just exceeds the target of B > 6.5; however, not all body segments meet this target. Some of the responses, particularly for the thorax, are close to scoring 10 points rating. The overall result is considered to be quite encouraging for a prototype dummy.

Table 14.
Summary ISOTR9790 Biofidelity Rating

Overall rating WorldSID 5th %-ile	
Head	10
Neck	4.9
Shoulder	5.0
Thorax	5.6
Abdomen	8.5
Pelvis	5.6
Overall rating	**6.7**

Repeatability

The repeatability of the dummy was evaluated by repeating the same test condition at least three times. Some of the results are presented in Table 15.Table 15. Table 17. In the Heidelberg sled test coefficients of variation were in the same order as in the WSU test.

Table 15.
WSU 6.8 m/s rigid sled internal measurement

Dummy segment	Magnitude	Mean	Sd	CV (%)
Thorax	T1 Acc. y (g)	45.3	1.8	4.0%
	T12 Acc. y (g)	68.6	5.2	7.6%
Ribs displacement [mm]	Shoulder	-59.1	0.25	0.4%
	Upper Thorax	44.5	2.1	4.6%
	Middle Thorax	47.3	0.7	1.5%
	Lower Thorax	44.7	1.5	3.4%
	Upper Abdomen	32.3	2.4	7.4%
	Lower Abdomen	10.5	2.4	23%
Pelvis	Acc. y (g)	78.9	1.3	1.7%
	Pubic Fy (N)	-1138	35	3.0%

Table 16.
WSU 6.8 m/s rigid sled external loads

Barrier beam	Mean	Sd	CV (%)
Shoulder Beam (N)	2772	98	3.5%
Thorax Beam (N)	4211	514	12.2%
Abdomen Beam (N)	2354	25	1.0%
Pelvis Beam (N)	7742	285	3.7%
Knee Beam (N)	10397	293	2.8%

Table 17.
14kg shoulder and thorax pendulum test

Parameter	Mean	Sd.	CV[%]
Shoulder deflection [mm]	24.6	1.0	4.1
Shoulder force [N]	2309	49	2.1
4.3m/s Thorax Rib 1 [mm]	15.9	0.3	1.6
4.3m/s Thorax Rib 2 [mm]	22.1	0.1	0.5
4.3m/s Thorax Rib 3 [mm]	20.2	0.2	1.1
4.3 m/s Pendulum force [N]	2678	25	0.9
4.3m/s T1 acceleration [G]	21.8	0.3	1.5
6.0m/s Thorax Rib 1 [mm]	26.9	1.2	4.5
6.0m/s Thorax Rib 2 [mm]	35.9	1.5	4.2
6.0m/s Thorax Rib 3 [mm]	34.0	1.2	3.6
6.0m/s Pendulum force [N]	3231	39	1.2

The WSU and Heidelberg padded test results were more repeatable then the rigid test results. Most results were well within the repeatability requirement of CV<7%. Some results do not meet the requirement. The CV of the thorax force beam in the WSU 6.8 m/s test was 12%. This result is attributed to differences in body segment contact orientation and timing due to differences in dummy sliding on the test bench. The high CV of the lower abdomen deflection was explained earlier in the paper. The pendulum tests are more repeatable then the sled tests.

Sensitivity

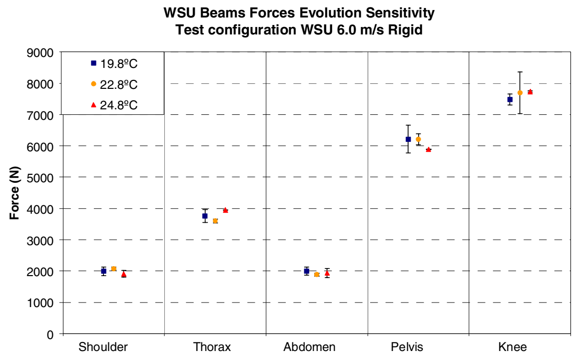

Figure 34. Temperature variation external measurements variability.

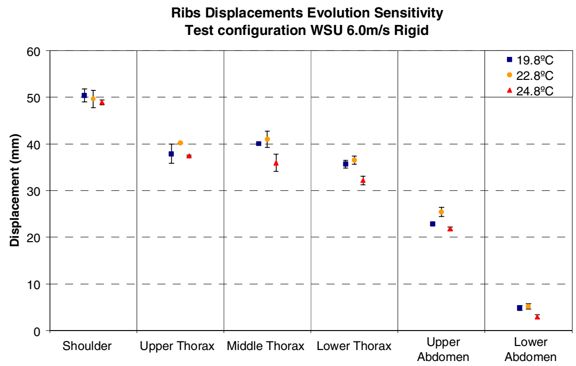

Figure 35. Temperature variation internal measurements variability.

Table 18
Variability of load responses

	Coefficient of variation (%)			
	Test 24.8ºC	Test 22.8ºC	Test 19.8ºC	All test 6.0 m/s
Shoulder Beam	4.02	1.55	4.72	4.70
Thorax Beam	0.00	1.23	3.99	4.59
Abdomen Beam	5.38	1.78	4.68	4.21
Pelvis Beam	0.12	2.06	5.05	3.70
Knee Beam	0.23	6.07	1.69	3.27

6.0m/s WSU sled tests were conducted at 20ºC, 23ºC and 25ºC environment temperature to evaluate the temperature sensitivity of the dummy. The results are shown in Figure 34 and Figure 35. The test results revealed no trends in dummy responses due to temperature variation. The variations due to temperature variation were below 5% and were similar to the test-to-test variability, see Table 18.

Dummy prototype problems

The main problems occurring during the Aprosys evaluation are given below.
Tilt sensor problems were experienced due to loss of software after the PDA battery had fully drained.
Dummy battery charging remained a problem, even after exchange of new batteries. No battery charge indicator is available to the user. Battery charge problems seem to be related to the long off time between charges as dummies were transported between labs.
Wiring problems were experienced. All of them can be attributed to the smaller size of the dummy and reduced space in the sternum and particularly in the pelvis, where wires were crushed and a connector was damaged in the 10.3 m/s Heidelberg tests. The prototype dummy pelvis had a high wire content with one pubic, two femur, two femoral neck, and double sacro-iliac load cells and a tri-axial accelerometer adding up to 40 channels.
Some signals registered by the in-dummy DAS system presented a high level of noise. It was found that the CAC settings were set to high for the expected data to be collected.
During the Aprosys evaluation the rib permanent deformation was monitored between tests. The thorax ribs were settling 1-2 mm and then remained constant. The shoulder sustained permanent deformation continuously until the rib width came closer to the thorax ribs, unloading the shoulder rib. In the 10.3 m/s rigid Heidelberg tests the thorax ribs also sustained permanent deformation, but no ribs were broken. Also the shoulder load cell connector sustained damage in this test. The shoulder rib stop appears not to be protecting the rib. The Heidelberg tests were run without IR traccs to avoid damage. In the WSU 6.8 rigid tests two IR traccs were damaged.

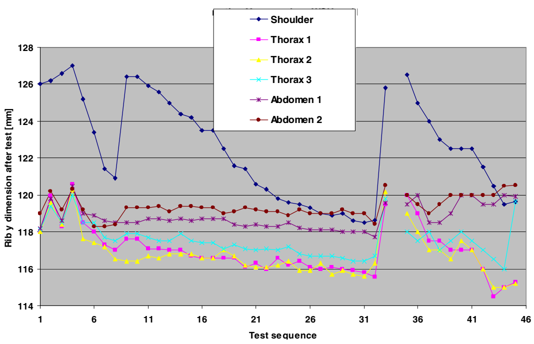

Figure 36. Rib permanent deformation record.

The IR-traccs in the thorax registered flat tops in the thorax compression (Figure 37). Also flat tops in the rib deflection were registered with the WorldSID small female dummy outside the Aprosys consortium.

The phenomena are believed to be related to forward deformation of the ribs relative to the spine and associated extension of the IR-traccs, (Hynd *et.al.* 2004). Flat top responses generally raise the concern whether the actual peak of the measured parameter is registered. Further, the IR-traccs are close to maximum range, even in moderate speed biofidelity tests.

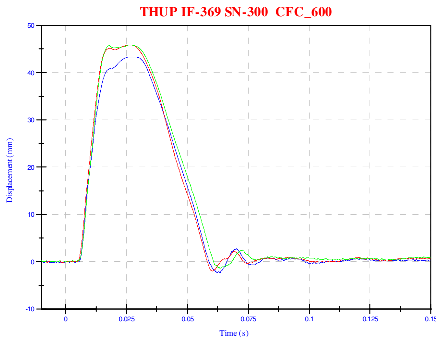

Figure 37. Upper rib deflection WSU 8.9 padded.

Also the shoulder deflection trace showed flat tops in the WSU tests. The shoulder string potentiometer is not recording the peak deflection, as shoulder rib accelerations exceeding 250 G were registered. The potentiometer is rated 50G, beyond which the string becomes slack.
Some problems were related to the half arm. The shoulder joint friction adjustment was difficult. The arm bone static bending stiffness of the dummy was compared analytically to human data based on Kemper *et.al.* (2005). The bending stiffness of the dummy humerus bone is much lower then the human target.

CONCLUSIONS and RECOMMENDATIONS

Conclusions

Two WorldSID small female prototype side impact dummies were extensively evaluated and tested to verify compliance of the dummy to its requirements. Some issues were found with the anthropometry, but these can be corrected. The overall biomechanical responses of the prototype just meets the target of good biofidelity (B>6.5), but not all body segments meet the biofidelity rating target. This is considered to be quite encouraging for a prototype dummy. However, some of the results are contradictory and do not provide clear guidance for improving the performance of the dummy . The repeatability of the dummy was good with a coefficient of variation generally below 5%. The sensitivity of the dummy to temperature variation was evaluated. The tests results revealed no trends in dummy responses in the temperature domain of the tests (20ºC -25ºC).

Recommendations for dummy update

Anthropometry - The abdomen and lower thorax mass shall be increased by 1.2kg. The lower leg should be redesigned to meet human anthropometry targets of mass, CoG location and target ratio of bone and flesh mass. The foot shall be redesigned to meet human anthropometry targets of mass and UMTRI surface shape and joint location. The half arm shall be redesigned to meet targets for total length, bone length and bone stiffness.

Biofidelity - The head skin thickness shall be tuned to meet the frontal impact response. The biofidelity targets for head-neck response appear to be conflicting and should be reviewed. The prediction of head injury as well as test data sample size should be prioritised when selecting biomechanical head-neck impact response specifications. Adopting the NBDL internal neck load corridors derived by Philippens *et al.* (2004) shall be considered.

Durability - Adequate fixation points for wires in the sternum and pelvis shall be provided. Wire lengths shall be optimised and wire gauge reduced if possible. Rib overload stops shall be designed for the shoulder and the thorax ribs.

Handling - The battery charging system shall be redesigned including a charge status indicator. The hip joint to iliac wing assembly shall be improved. The shoulder joint friction adjustment shall be improved.

Instrumentation - A rib deflection measurement system shall be developed to meet the following targets: 2d measurement of deflection in the rib plane; increased range of measurement exceeding 60mm; suitable for implementation in the shoulder, thorax and abdomen; suitable to act as rib overload protector.

Procedures - Pubic load shall be well controlled, as it is an injury assessment parameter. The certification procedure shall be updated to include pubic load measurement.

ACKNOWLEDGEMENTS

This work was supported through funding from: the European Commission, UK Department for Transport, MEC, DGUI-SEGVAUTO, and Dutch Ministry of Transport, Public Works and Water Management. In- dummy data acquisition system: DTS; Accelerometers: AUDI AG; Staff of test laboratories FTSS - INRETS - TNO - TRL - UMP-INSIA.

REFERENCES

Barnes A.S., Been B.W., Bermond F., Bortenschlager K., Caire Y., Carrol J.A., Compigne S., Hynd D. and Martinez L. (2004). "WorldSID 5th Female Requirements", APROSYS Document number AP-SP52 0007-D1.

Hynd D., Carrol J.A., BeenB.W. and Payne A.R., "Evaluation of the Shoulder Thorax and Abdomen of the WorldSID Pre-Production Side Impact Dummy", IMechE Vehicle Safety Conference 2004.

Irwin A.L., Mertz H.J., Ali M. Elhagediab A.M. and Moss S. (2002). "Guidelines for Assessing the Biofidelity of Side Impact Dummies of Various Sizes and Ages", SAE 2002-22-0016, Stapp Car Crash Journal, Vol. 46 November 2002, pp 297-319.

ISO (1997). ISO/TC22/SC12/WG5, Road Vehicles – Anthropometric side impact dummy – Lateral impact response requirements to assess the biofidelity, Technical Report 9790.

Kemper A., Stitzel J., Duma S., Matsuoka F. and Masuda M., "Biofidelity of the SID-IIs and a modified SID-IIs upper extremity: Biomechanical properties of the human humerus", Paper Number 05-0123.

Philippens M., Cappon H., and van Ratingen M., "Human volunteer head-T1 response for oblique impact conditions", International IRCOBI Conference on the Biomechanics of Impact. Graz, Austria, 2004.

Roberts A., Lowne R., Beusenberg M. and Cesari D. (1991). "Test procedures for defining biofidelity targets for lateral impact test dummies" 13th International Conference on Experimental Safety Vehicles, Paris, France, 04th to 07th November, 1991.

Schneider L.W., Robbins D.H, Pflüg M.A. and Snyder R.G. (1983). "Development of anthropometrically based design specifications for an advanced adult anthropomorphic dummy family." Final Report DOT-HS-806-715 NHTSA.

Wang Z.J., Been, B.W., Barnes A.S., Burleigh M.J., Schmidt A., Dotinga M. and Ratingen M.R.van (2007). "WorldSID 5th Percentile Prototype Dummy Development", SAE #2007-01-0701.